HAL
open science

Gravitational birefringence and an exotic formula for redshift

Christian Duval, Johanna Pasquet, Thomas Schucker, Andre Tilquin

To cite this version:

Christian Duval, Johanna Pasquet, Thomas Schucker, Andre Tilquin. Gravitational birefringence and an exotic formula for redshift. Physical Review D, 2018, 97 (12), pp.123508. 10.1103/PhysRevD.97.123508 . hal-01772665

HAL Id: hal-01772665

https://hal.science/hal-01772665v1

Submitted on 20 Apr 2018

HAL is a multi-disciplinary open access archive for the deposit and dissemination of scientific research documents, whether they are published or not. The documents may come from teaching and research institutions in France or abroad, or from public or private research centers.

L'archive ouverte pluridisciplinaire **HAL**, est destinée au dépôt et à la diffusion de documents scientifiques de niveau recherche, publiés ou non, émanant des établissements d'enseignement et de recherche français ou étrangers, des laboratoires publics ou privés.

Gravitational birefringence and an exotic formula for redshift

Christian Duval[1], Johanna Pasquet[2], Thomas Schücker[3] and André Tilquin[4]

Abstract

We compute the birefringence of light in curved Robertson-Walker spacetimes and propose an exotic formula for redshift based on the internal structure of the spinning photon. We then use the Hubble diagram of supernovae to test this formula.

PACS: 98.80.Es, 98.80.Cq
Key-Words: cosmological parameters – supernovae
1802.09295

[1] Aix-Marseille University, Université de Toulon, CPT, Marseille, France
supported by the ARCHIMED Labex (ANR-11-LABX-0060) funded by the "Investissements d'Avenir" French government program
christian.duval@cpt.univ-mrs.fr

[2] Aix-Marseille University, CPPM, Marseille, France
supported by the OCEVU Labex (ANR-11-LABX-0060) funded by the "Investissements d'Avenir" French government program
pasquet@cppm.in2p3.fr

[3] Aix-Marseille University, Université de Toulon, CPT, Marseille, France
supported by the ARCHIMED Labex (ANR-11-LABX-0060) funded by the "Investissements d'Avenir" French government program
thomas.schucker@gmail.com

[4] Aix-Marseille University, CPPM, Marseille, France
supported by the OCEVU Labex (ANR-11-LABX-0060) funded by the "Investissements d'Avenir" French government program
tilquin@cppm.in2p3.fr

1 Introduction

Birefringence of light in absence of anisotropic material but in presence of a reflecting surface, was predicted by Federov [6] in 1955 and by Imbert [9] in 1972. It implies an offset of the order of a wavelength between the outgoing photons of either circular polarisation. In 2008 this was indeed observed [2, 8].

Birefringence of light in presence of the gravitational field of the Schwarzschild metric was computed by Saturnini [17] in 1976 and recently by two of us [5] in a flat Robertson-Walker metric.

In the second case, the photons follow helical trajectories whose chirality is given by the two circular polarisations. The distance between the two trajectories at arrival is – as in the Fedorov-Imbert effect – of the order of a wavelength but direct observation of this offset seems much more difficult.

The period of the helix is equal to the period of spin precession and depends on the atomic period of the photon. But it also depends on the acceleration of the universe. This 'internal structure' of the spinning photon encourages us to propose an exotic definition of redshift based on the precession period rather than on the atomic period.

The aim of this paper is two-fold. First, we generalise our computations of reference [5] from flat to curved Robertson-Walker metrics, sections 2 and 3, and present the resulting exotic definition of redshift, section 4. Second, in a universe filled with cold matter only, we confront our exotic definition to the Hubble diagram of supernovae, section 5 with the initial hope that the acceleration dependence in the exotic redshift might yield a good fit with less (dark) matter.

2 Theory

Consider the wordline $X(\tau)$ of a massless particle with non-vanishing spin in a gravitational field described by a metric g. Denote by $P(\tau)$ the 4-momentum of the particle and by $S(\tau)$ its spin tensor (viewed as a linear map). The wordline is determined by the Souriau-Saturnini equations [10, 4, 19, 17], which are obtained from the Mathisson-Papapetrou-Dixon equations [11, 12, 20, 3, 4, 19] by setting $SP = 0$. This constraint implies that P^2 and the 'scalar spin' s defined by $s^2 := -\frac{1}{2}\mathrm{Tr}(S^2)$ are both constants of motion. For the photon of course we set:

$$P^2 = 0\,, \qquad s = \pm\hbar\,. \tag{2.1}$$

Then the Souriau-Saturnini equations read:

$$\dot{X} = P + \frac{2}{R(S)(S)} SR(S)P\,, \tag{2.2}$$

$$\dot{P} = -s\,\frac{\mathrm{Pf}(R(S))}{R(S)(S)}\,P\,, \tag{2.3}$$

$$\dot{S} = P\overline{\dot{X}} - \dot{X}\overline{P}. \tag{2.4}$$

Our conventions are: $\dot{X}^\mu := dx^\mu/d\tau$, $(\mu = 1\,,2\,,3\,,4)$ and $(\overline{P})_\nu := g_{\nu\mu}P^\mu$. Over P and S, the dot denotes the covariant derivative with respect to τ. $R(S)(S) := -\mathrm{Tr}(SR(S)) := R_{\mu\nu\alpha\beta}\,S^{\mu\nu}S^{\alpha\beta}$.

Of course we must assume $R(S)(S) \neq 0$. In (2.3), the Pfaffian of the skewsymmetric linear map $F = R(S)$ is such that $\star(F)F = \mathrm{Pf}(F)\,\mathbf{1}$, where $\star$ is the Hodge star; we have $\det(F) = -\mathrm{Pf}(F)^2$. Note that $\mathrm{Pf}(F) = -\frac{1}{8}\sqrt{-\det(\mathrm{g}_{\alpha\beta})}\,\varepsilon_{\mu\nu\rho\sigma}F^{\mu\nu}F^{\rho\sigma}$ with $\varepsilon_{\mu\nu\rho\sigma}$ the Levi-Civita symbol such that $\varepsilon_{1234} = 1$.

The Souriau-Saturnini equations also imply that 4-momentum and 4-velocity are orthogonal, $\overline{P}\dot{X} = 0$.

Let us write the Robertson-Walker metric with respect to the Euclidean coordinates $\mathbf{x}$ of $\mathbb{R}^3$ after stereographic projection and with respect to cosmic time t:

$$\mathrm{g} = -a(t)^2\,\frac{\|d\mathbf{x}\|^2}{b(\mathbf{x})^2} + dt^2 \quad \text{with} \quad b(\mathbf{x}) := 1 + \frac{K}{4}\|\mathbf{x}\|^2. \tag{2.5}$$

Our conventions are such that the curvature scalar of 3-space is $6K$. The Euclidean coordinates will come in handy because of frequent vector products.

In these coordinates we write the momentum of the particle as

$$P = \begin{pmatrix} \frac{b}{a}\mathbf{p} \\ \|\mathbf{p}\| \end{pmatrix} \tag{2.6}$$

with 3-momentum $\mathbf{p}$ and *positive* energy $\|\mathbf{p}\| := \sqrt{\mathbf{p}\cdot\mathbf{p}}$. Accordingly, we write the spin $(1,1)$-tensor as

$$S = \begin{pmatrix} j(\mathbf{s}) & -\frac{(\mathbf{s}\times\mathbf{p})}{\|\mathbf{p}\|}\frac{b}{a} \\ -\frac{(\mathbf{s}\times\mathbf{p})^T}{\|\mathbf{p}\|}\frac{a}{b} & 0 \end{pmatrix}. \tag{2.7}$$

Transposition is denoted by a superscript $\cdot^T$ and we use $j(\mathbf{s})\colon \mathbf{p} \mapsto \mathbf{s}\times\mathbf{p}$. The relation between the scalar spin and the spin vector $\mathbf{s} \in \mathbb{R}^3 \setminus \{0\}$ then reads

$$s = \frac{\mathbf{s}\cdot\mathbf{p}}{\|\mathbf{p}\|} \tag{2.8}$$

and we find

$$R(S) = -\frac{2}{a^2}\begin{pmatrix} (K + a'^2)j(\mathbf{s}) & -\frac{\mathbf{s}\times\mathbf{p}}{\|\mathbf{p}\|}\,b\,a'' \\ -\frac{(\mathbf{s}\times\mathbf{p})^T}{\|\mathbf{p}\|}\,\frac{a^2a''}{b} & 0 \end{pmatrix}, \tag{2.9}$$

together with $\det(R(S)) = 0$ implying that the 4-momentum P is parallel-transported.

Furthermore we have

$$R(S)(S) = \frac{4}{a^2}\left(\|\mathbf{s}\|^2(aa'' - (K + a'^2)) - s^2\,aa''\right). \tag{2.10}$$

and

$$SR(S)P = \frac{2}{a^2}((K + a'^2) - aa'')\left(\|\mathbf{s}\|^2 P - s\,W\right) \tag{2.11}$$

with the 'Pauli-Lubanski' vector

$$W := \|\mathbf{p}\| \begin{pmatrix} \frac{b}{a}\mathbf{s} \\ s \end{pmatrix} \tag{2.12}$$

interpreted as the *polarization vector* of the massless particle in the gravitational field.

Next we trade the curve parameter τ for the cosmic time. The fourth component of Equation (2.2),

$$\frac{dt}{d\tau} = -\frac{4s^2\|\mathbf{p}\|}{R(S)(S)}\frac{(K+a'^2)}{a^2}\,, \tag{2.13}$$

tells us that we must assume $R(S)(S) \neq 0$, as already noted, but also $K + a'^2 \neq 0$. Then we can write

$$\frac{dX}{dt} = \frac{aa''}{\|\mathbf{p}\|(K+a'^2)}\left[P - \left(1 - \frac{K+a'^2}{aa''}\right)\frac{W}{s}\right]\,, \tag{2.14}$$

where the Pauli-Lubanski vector W features the polarization-driven 'anomalous velocity'.

Let us write the *de*celeration parameter modified by curvature as

$$Q(t) := -a(t)a''(t)/(K + a'(t)^2)\,. \tag{2.15}$$

Then the equations of motion read in our $3+1$ decomposition:

$$\frac{d\mathbf{x}}{dt} = \frac{b}{a}\left[-Q\frac{\mathbf{p}}{\|\mathbf{p}\|} + (1+Q)\,\frac{\mathbf{s}}{s}\right], \tag{2.16}$$

$$\begin{aligned}\frac{d\mathbf{p}}{dt} &= -\frac{a'}{a}\left[-Q\,\mathbf{p} + \|\mathbf{p}\|\,(1+Q)\,\frac{\mathbf{s}}{s}\right] \\ &\quad + \frac{K}{2a}\left[(1+Q)\,(\mathbf{p}\cdot\mathbf{x})\frac{\mathbf{s}}{s} - Q\frac{(\mathbf{p}\cdot\mathbf{x})}{\|\mathbf{p}\|}\,\mathbf{p} - \|\mathbf{p}\|\,\mathbf{x}\right],\end{aligned} \tag{2.17}$$

$$\begin{aligned}\frac{d\mathbf{s}}{dt} &= -\,(1+Q)\,\frac{\mathbf{s}}{s}\times\mathbf{p} - \frac{a'}{a}\left[\mathbf{s} + \left[s\,Q - (1+Q)\,\frac{\|\mathbf{s}\|^2}{s}\right]\frac{\mathbf{p}}{\|\mathbf{p}\|}\right] \\ &\quad + \frac{K}{2a}\left[(1+Q)\frac{\mathbf{s}}{s}\times(\mathbf{s}\times\mathbf{x}) - \,Q\left[(\mathbf{s}\cdot\mathbf{x})\frac{\mathbf{p}}{\|\mathbf{p}\|} - s\,\mathbf{x}\right]\right].\end{aligned} \tag{2.18}$$

With $b_\pm := 1 \pm \frac{K}{4}\|\mathbf{x}\|^2$ (implying $b = b_+$) and defining the transverse spin

$$\mathbf{s}^\perp := \mathbf{s} - s\frac{\mathbf{p}}{\|\mathbf{p}\|}\,, \tag{2.19}$$

we have the following constants of motion:

$$\begin{aligned}
\mathcal{P} &= \frac{b_-}{b_+}\left[a\,\mathbf{p} + a'\mathbf{s}\times\frac{\mathbf{p}}{\|\mathbf{p}\|}\right] \\
&\quad + \frac{K}{2b_+}\left[2\,\mathbf{x}\times\mathbf{s} + \left[a'\,\mathbf{x}\cdot\left(\mathbf{s}\times\frac{\mathbf{p}}{\|\mathbf{p}\|}\right) + a\,(\mathbf{x}\cdot\mathbf{p})\right]\mathbf{x}\right], \qquad (2.20)\\
\mathcal{L} &= \frac{1}{b_-}\left[\mathbf{x}\times\mathcal{P} + b_+\,\mathbf{s} - \frac{K}{2}(\mathbf{s}\cdot\mathbf{x})\,\mathbf{x}\right], \qquad (2.21)\\
\mathcal{E} &= a\,\|\mathbf{p}\|\,, \qquad (2.22)\\
s &= \frac{\mathbf{s}\cdot\mathbf{p}}{\|\mathbf{p}\|}\,, \qquad (2.23)\\
\mathcal{S} &= \sqrt{K + a'^2}\,\|\mathbf{s}^\perp\|\,. \qquad (2.24)
\end{aligned}$$

As detailed for the flat case in reference [5] the conservation of momentum $\mathcal{P}$ and angular momentum $\mathcal{L}$ follows from the invariance of the Robertson-Walker metric (2.5) under infinitesimal "translations" and rotations

$$\delta\mathbf{x} = \boldsymbol{\omega}\times\mathbf{x} + \boldsymbol{\alpha}\,b_- + \frac{K}{2}\mathbf{x}(\mathbf{x}\cdot\boldsymbol{\alpha}) \qquad (2.25)$$

with $\boldsymbol{\alpha},\boldsymbol{\omega}\in\mathbb{R}^3$. The conservation of energy $\mathcal{E}$ comes from the *conformal* Killing vector $a(t)\,\partial/\partial t$. Generalizing the proof of the conservation of transverse spin $\mathcal{S}$ from [5] to the curved case is difficult and we give an alternative one, starting with

$$\frac{d}{dt}\left(\frac{1}{2}||\mathbf{s}||^2\right) = \frac{d}{dt}\left(\frac{1}{2}||\mathbf{s}^\perp||^2\right) = \mathbf{s}\cdot\frac{d\mathbf{s}}{dt} = Q\,\frac{a'}{a}\,||\mathbf{s}^\perp||^2. \qquad (2.26)$$

Here we have used the equation of motion for the spin vector (2.18) and the relation between the scalar spin and the spin vector (2.8). With the definition of the deceleration parameter, $Q = -aa''/(K + a'^2)$, we finally obtain $d/dt[(K + a'^2)||\mathbf{s}^\perp||^2] = 0$.

As already in the flat case [5] we can use the constants of motion to express the spin vector as a function of momentum and position:

$$\mathbf{s} = \frac{1}{b_+}\left[b_-\,\mathcal{L} + \frac{K}{2}(\mathbf{x}\cdot\mathcal{L})\,\mathbf{x} - \mathbf{x}\times\mathcal{P}\right]. \qquad (2.27)$$

However the analogous simple expression for the momentum, that we enjoyed in the flat case, equation (4.4) of reference [5], eludes us for non-vanishing curvature K.

Using the constants of motion we can rewrite Equation (2.10):

$$R(S)(S) = -\frac{4}{a^2}\left(\|\mathcal{S}\|^2(1+Q) + s^2\,(K + a'^2)\right), \qquad (2.28)$$

which must never vanish.

Let us anticipate that later on we will have to assume that $1+Q$ alone never vanishes. Therefore we need to verify both constraints $1+Q>0$ and $K+a'^2>0$ independently at any time. They can be recast conveniently using the Friedman equations in presence of a single matter component with energy density ρ and with vanishing pressure. With the usual dimensionless cosmological parameters,

$$\Omega_\Lambda := \frac{\Lambda}{3H^2}\,, \quad \Omega_k := \frac{-K}{a^2H^2}\,, \quad \Omega_m := \frac{8\pi G\,\rho}{3H^2}\,, \tag{2.29}$$

we find that $1+Q>0$ if and only if $\Omega_\Lambda+\Omega_k<1$ or equivalently $\Omega_m>0$ and $K+a'^2>0$ if and only if $\Omega_k<1$ or equivalently $\Omega_m+\Omega_\Lambda>0$.

3 Perturbation

We would like to solve the equations of motion (2.16 - 2.18) with initial conditions at $t=t_e$, the time of emission:

$$\mathbf{x}_e = 0, \quad \mathbf{p}_e = \begin{pmatrix} \|\mathbf{p}_e\| \\ 0 \\ 0 \end{pmatrix}, \quad \mathbf{s}_e = \begin{pmatrix} s \\ s_e^\perp \\ 0 \end{pmatrix} \tag{3.1}$$

with $s_e^\perp := \|\mathbf{s}_e^\perp\| \geq 0$. For 'enslaved spin', $s_e^\perp = 0$, we retrieve the null geodesics: $x^1=\tilde{x}$, $p_1 = a(t_e)/a(t)\,\|\mathbf{p}_e\|$, $s_1 = s$ with

$$\tilde{x}(t) := \begin{cases} 2/\sqrt{|K|}\,\tan\left(\sqrt{|K|}/2\,\int_{t_e}^t d\tilde{t}/a(\tilde{t})\right) & K>0 \\ \int_{t_e}^t d\tilde{t}/a(\tilde{t}) & K=0 \\ 2/\sqrt{|K|}\,\tanh\left(\sqrt{|K|}/2\,\int_{t_e}^t d\tilde{t}/a(\tilde{t})\right) & K<0 \end{cases} \tag{3.2}$$

and the six other components vanish.

We will be dealing with two small parameters, typically of the order of 10^{-33},

$$\eta := \frac{s}{\mathcal{E}}\,, \qquad \epsilon := \frac{s_e^\perp}{\mathcal{E}} \tag{3.3}$$

We consider η to be a fixed, non-zero number and ϵ to vary between 0 and $|\eta|$. Indeed we know that for $\epsilon=0$ our trajectory is the null geodesic and we want to know how the trajectory of the photon deviates from this geodesic to first order in ϵ. At the end of our calculation we will put $\epsilon=|\eta|$ for the photon.

From numerical solutions in the flat case $K=0$, we know that the six components, which vanish for vanishing ϵ, are at least of first order in ϵ justifying the Ansatz:

$$\mathbf{x} = \begin{pmatrix} \tilde{x}+\epsilon y_1 \\ \epsilon y_2 \\ \epsilon y_3 \end{pmatrix}, \quad \frac{\mathbf{p}}{\mathcal{E}} = \begin{pmatrix} 1/a+\epsilon q_1 \\ \epsilon q_2 \\ \epsilon q_3 \end{pmatrix}, \quad \frac{\mathbf{s}}{\mathcal{E}} = \begin{pmatrix} \eta+\epsilon r_1 \\ \epsilon r_2 \\ \epsilon r_3 \end{pmatrix}. \tag{3.4}$$

Computing $\|\mathbf{p}/\mathcal{E}\|^2$ we immediately find that $q_1 \sim 0$. Likewise we compute

$$s/\mathcal{E} = \left(\frac{\mathbf{p}}{\mathcal{E}} \cdot \frac{\mathbf{s}}{\mathcal{E}}\right) / \frac{\|\mathbf{p}\|}{\mathcal{E}} \tag{3.5}$$

with our Ansatz and find that $r_1 \sim 0$. Now consider the spin divided by $\mathcal{E}$ written in terms of the constants of motion, equation (2.27), and replace the constants of motion by the initial values and replace $\mathbf{x}$ by our Ansatz. Then we get to first order in ϵ:

$$r_2 \sim \frac{b_- - a_e'\tilde{x}}{b_+} - \frac{y_3}{b_+}\,, \tag{3.6}$$

$$r_3 \sim \frac{y_2}{b_+}\,. \tag{3.7}$$

Finally we use equation (2.20) and write the vector of constants of motion $\mathcal{P}/\mathcal{E}$ for $t = t_e$ and for arbitrary t using the Ansatz. The first component is fulfilled identically to first order. The other two components yield

$$q_2 \sim \left[-\frac{a'}{ab_+} + \frac{K\tilde{x}}{2ab_-}\left(\frac{2}{b_+} - 1\right)\right] y_2, \tag{3.8}$$

$$q_3 \sim -\frac{a_e' b_+}{ab_-} + \frac{a' b_-}{ab_+} - \frac{a_e' a' \tilde{x}}{ab_+} - \frac{K\tilde{x}}{ab_+} + \frac{a_e' K \tilde{x}^2}{ab_+ b_-} + \left[-\frac{a'}{ab_+} + \frac{K\tilde{x}}{2ab_-}\left(\frac{2}{b_+} - 1\right)\right] y_3. \tag{3.9}$$

We are now ready to linearize the 3-velocity (2.16):

$$\frac{dx_1}{dt} \sim \frac{b}{a} \qquad \text{implying} \qquad \frac{dy_1}{dt} = 0, \tag{3.10}$$

$$\frac{dy_2}{dt} \sim -Q\,b\,q_2 + \frac{1+Q}{a}\,b\,\frac{1}{\eta}\,r_2 \sim \frac{1+Q}{\eta a}\left[-y_3 + b_- - a_e'\tilde{x}\right], \tag{3.11}$$

$$\frac{dy_3}{dt} \sim -Q\,b\,q_3 + \frac{1+Q}{a}\,b\,\frac{1}{\eta}\,r_3 \sim \frac{1+Q}{\eta a}\left[+y_2\right]. \tag{3.12}$$

Since $y_1(t_e) = 0$, we conclude that y_1 vanishes everywhere. Note that the momenta q_2 and q_3 do not contribute in leading order. Let us suppose that $1+Q$ does not vanish between emission time t_e and today t_0. Then we may define a new time coordinate θ by:

$$\frac{d\theta}{dt} = \frac{1}{|\eta|}\,\frac{1+Q}{a} \qquad \text{and} \qquad \theta(t_e) = 0, \tag{3.13}$$

and new dependent variables $\tilde{z}(\theta) := \tilde{x}(t(\theta))$, $z_2(\theta) := y_2(t(\theta))$ and $z_3(\theta) := y_3(t(\theta))$. Then we have:

$$\frac{dz_2}{d\theta} \sim \text{sign}(\eta)[-z_3 + b_- - a_e'\,\tilde{z}], \tag{3.14}$$

$$\frac{dz_3}{d\theta} \sim \text{sign}(\eta)\,z_2\,. \tag{3.15}$$

Setting $\epsilon = |\eta| = T_e/(2\pi\, a_e)$, the solution is $z_2 \sim \mathrm{sign}(\eta)\, \sin\theta$ and $z_3 \sim -\cos\theta - 1 + a_e' \tilde{z}$, a helix of constant period 2π with respect to the time coordinate θ. The period is variable with respect to cosmic time:

$$T_{\mathrm{helix}}(t) \sim \frac{a(t)}{a_e} \frac{1}{1+Q(t)} T_e, \tag{3.16}$$

where T_e is the atomic period of the light (spin 1) at emission. The radius of the helix is also time dependent:

$$R_{\mathrm{helix}}(t) \sim \frac{a(t)}{a_e} \frac{1}{1+K\tilde{x}(t)^2} \lambda_e, \tag{3.17}$$

where $\lambda_e = c\, T_e$ is the wavelength of the light at emission. To leading order, the center of the helix has comoving coordinates

$$\begin{pmatrix} \tilde{x}(t) \\ 0 \\ T_e/(2\pi\, a_e)\ [1 - a_e'\, \tilde{x}(t) - K\tilde{x}(t)^2] \end{pmatrix}. \tag{3.18}$$

4 An exotic definition of redshift

Taking due account of its spin, the photon propagates through a Robertson-Walker universe on a helix and we wonder if Feynman already knew about this when he chose to represent the photon propagator by a curly line.

Of course the main question is whether the offset between two helices of opposite polarisation, 'birefringence', is observable today. The offset is to oscillate between 0 and $2\, R_{\mathrm{helix}}(t_0)$ with a period of $\frac{1}{2} T_{\mathrm{helix}}(t_0)$, where $T_{\mathrm{helix}}(t)$ is the period of the helix and at the same time it is the period of precession of the spin vector $\mathbf{s}$ around its direction of mean propagation.

Thanks to its spin, the photon carries two informations (besides its direction):

- The first information is the well measured **atomic period** today T_0, which is related to the atomic period at emission T_e by

  $$T_0 = \frac{a(t_0)}{a(t_e)} T_e. \tag{4.1}$$

  This relation has two derivations: In the classical one, we compute the cosmic times of flight of a photon emitted by a co-moving source at time t_e and arriving at a co-moving observer at time t_0 and of a second photon emitted at time $t_e + T_e$ by the same co-moving source and arriving at the same co-moving observer at time $t_0 + T_0$. We note that cosmic time is equal to proper time for both source and observer. The second derivation is quantum, as it uses de Broglie's relation between the atomic period T_e and the energy $\|\mathbf{p}_e\|$ of the emitted photon. It also uses the conserved 'energy' $\mathcal{E} = a\|\mathbf{p}_e\|$, Equation (2.22).

  This harmony between de Broglie's relations and general relativity has been verified experimentally for the first time in 1960 in the (static) gravitational field of the Earth at Harvard by Pound and Rebka [13].

- The photon carries a second information, its **period of precession** today $T_{\text{helix}}(t_0) =: T_{\text{helix}\,0}$ which is related to its atomic period T_0 today by

$$T_{\text{helix}\,0} \;=\; \frac{1}{1+Q(t_0)}\,T_0\,. \tag{4.2}$$

  The derivation, presented above, also involves the conserved 'angular momentum' $\mathcal{L}$ and 'spin' $\mathcal{S}$ and s.

While waiting for a direct observation of birefringence, Equation (4.2) invites us to be bold and (ignoring the mentioned harmony) assume that, when telling us their redshift, photons use the second information they carry, $z = (T_{\text{helix}\,0} - T_{\text{helix}\,e})/T_{\text{helix}\,e}$, and not the first one, $z = (T_0 - T_e)/T_e$, which we must assume when we ignore spin.

This assumption leads to an exotic formula for the redshift,

$$z+1 \;=\; \frac{a(t_0)}{a(t_e)}\,\frac{1+Q(t_e)}{1+Q(t_0)}\,, \tag{4.3}$$

which differs substantially from the standard formula by the presence of the modified deceleration parameter Q.

Let us otherwise remain conservative and assume that gravity is well described by general relativity up to cosmic scales. We also assume the cosmological principle, i.e. that at cosmic scales our universe is maximally symmetric, and that supernovae of type Ia are standardizable candles. Then using again the conserved 'energy' $\mathcal{E} = a\|\mathbf{p}_e\|$, the apparent luminosity is given by

$$\ell \;=\; \frac{L}{4\pi\,a_0^2}\,\frac{1}{\text{si}^2(t_0)}\,\frac{a_e^2}{a_0^2}\,, \tag{4.4}$$

where L is the absolute luminosity of the supernova and

$$\text{si}(t) := \begin{cases} 1/\sqrt{|K|}\,\sin\left(\sqrt{|K|}\,\int_{t_e}^{t} d\tilde{t}/a(\tilde{t})\right) & K>0 \\ \int_{t_e}^{t} d\tilde{t}/a(\tilde{t}) & K=0 \\ 1/\sqrt{|K|}\,\sinh\left(\sqrt{|K|}\,\int_{t_e}^{t} d\tilde{t}/a(\tilde{t})\right) & K<0 \end{cases}\,. \tag{4.5}$$

We are now ready to confront our exotic formula with the Hubble diagram of supernovae.

5 Observation

We use the 740 type Ia supernovae from the Joint Light Curve Analysis (JLA) [1]. The JLA published data provide the observed uncorrected peak magnitude (m_{peak}), the time stretching of the light-curve ($X1$) and color (C) at maximum brightness due to intrinsic supernovae property and extinction by dust in the host galaxy. These quantities are estimated in the restframe of each supernova by the SALT2 empirical model of Type Ia supernovae spectro-photometric evolution with time trained on the whole supernovae sample [7].

The reconstructed magnitude after the SALT2 fitting procedure reads:

$$m_r = m_{\text{peak}} + \alpha_s X1 - \beta_c C, \tag{5.1}$$

where α_s and β_c are global parameters fitted to the Hubble diagram simultaneously with all the other parameters. The expected magnitude can be simply written as:

$$m_e = m_s - 2.5\, log_{10}\, \ell(a(t_e))\,, \tag{5.2}$$

where $\ell(a(t_e))$ is given by (4.4) and m_s a global normalisation parameter.

Because of the new relation between observed redshift and scale factor at emission (4.3) the restframe of each supernovae is at a different emission time compared to the one given by the standard redshift. Thus, the global light curve fit must be redone.

Using both Friedmann equations for a non flat Universe, and setting $a(t_0) = 1$ the new observed redshift reads:

$$z + 1 \;=\; \frac{1}{a(t'_e)}\,\frac{\Omega_{m0} + \Omega_{\Lambda 0}}{\Omega_{m0} + \Omega_{\Lambda 0}\, a(t'_e)^3}\,, \tag{5.3}$$

where t'_e is the new photon emission time and (Ω_{m0}, $\Omega_{\Lambda 0}$) the cosmological parameters today.

Consequently the scale factor at emission $a(t'_e)$ for a given observed redshift is now a function of the cosmological model. For a positive cosmological constant, the correction factor is always greater than one which implies that supernovae appear to be closer to us. Notice that for a vanishing cosmological constant the exotic redshift is similar to the standard one.

We use a numerical gradient method to invert (5.3) with a minimum step in scale factor well below the associated experimental redshift error. This new scale factor $a(t'_e)$ is then used as input to the SALT2 public software through a new effective redshift for each supernova:

$$z_{\text{eff}} + 1 := 1/a(t'_e)\,. \tag{5.4}$$

The SALT2 fitting procedure returns new values for m_{peak}, $X1$ and C as well as the full covariance matrix between those parameters. Finally the JLA public likelihood software is used to compute the general χ^2 expressed in terms of the full covariance matrix including correlations and systematics. It reads

$$\chi^2 = \Delta M^T V^{-1} \Delta M, \tag{5.5}$$

where ΔM is the vector of differences between the expected supernova magnitudes m_e and the reconstructed experimental magnitudes at maximum of the light curve m_r. The minimisation of the χ^2 is preformed with the MINUIT minimizer software [14].

Figure 1-a shows the Hubble diagram for both redshift definitions. The black points are the reconstructed magnitude at peak for the standard redshift definition and the black curve corresponds to the global fit on all parameters (m_s, α_s, β_c, Ω_{m0}, $\Omega_{\Lambda 0}$). The red points are the reconstructed magnitudes given by the SALT2 light curve refitting using the new redshift definition with the same standard fiducial cosmology and calibrated at the same low redshift value where both redshift definitions are identical. The red curve is obtained by refitting only

(m_s, α_s, β_c). These two curves and the set of points show the important effect of the light curve refitting on the reconstructed magnitude. This is better seen in figure 1-b which shows the reconstructed magnitude difference m_r(standard)$-m_r$(exotic) due to the light curve refitting with the exotic redshift. We estimate the intrinsic magnitude dispersion as the square root of the mean square between curves and points: $\sigma_{intrinsic}$(standard)$= 0.17$ and $\sigma_{intrinsic}$(exotic)$= 0.27$. The standardization of supernova magnitudes with the exotic redshift is worse than with the standard one.

For completness, table 1 shows the results of the full fit with the standard redshift (line 1) and of the partial fit with the exotic redshift assuming the same fiducial cosmology (line 2) corresponding respectively to black and red curves in figure 1-a. The high χ^2 value of line 2 is a consequence of the partial refit done at the same fiducial cosmology. This is why we have to do a global refit (shown in line 3).

Redshift	α_s	β_c	Ω_{m0}	$\Omega_{\Lambda 0}$	χ^2
Standard	0.138 ± 0.006	3.14 ± 0.08	0.22 ± 0.11	0.63 ± 0.16	748.9
Exotic (partial fit)	0.099 ± 0.005	1.58 ± 0.02	fixed to 0.22	fixed to 0.63	1609
Exotic (refit)	0.137 ± 0.006	3.16 ± 0.08	-0.15 ± 0.07	$(-3 \pm 2)10^{-4}$	757.6

Table 1: 1 σ errors for stretch, color and cosmological parameter fits. Line 1 corresponds to the standard redshift, line 2 to the exotic redshift after refitting light curves but at the same fiducial cosmology than line 1. Line 3 corresponds to the global fit using exotic redshift and light curve refitting.

To find the true minimum with the exotic redshift we face a new problem: we cannot use the standard minimization method MINUIT due to numerical instabilities in the light curve fit for all cosmologies. Indeed, MINUIT requires first numerical derivatives of the χ^2 with respect to Ω_{m0} and $\Omega_{\Lambda 0}$ which lead to many fake minima.

To overcome this problem we prefer to explore the Ω_{m0}, $\Omega_{\Lambda 0}$ parameter space using an accurate grid of points. At each point the SALT2 fit is performed on light curves using the effective redshift and the output is used to minimize the χ^2 with respect to all other parameters using the JLA standard likelihood and MINUIT. To avoid any a priori about the final result and despite the fact that both constraints $1 + Q > 0$ and $K + a'^2 > 0$ are not fulfilled, we decided to explore Ω_{m0} from -1 to 1 and $\Omega_{\Lambda 0}$ from -1 to 3 on a grid of about 30.000 points. This required three and a half CPU years made available to us by the Dark Energy Center [5]. After identifying the true minimum, we explored more accurately the χ^2 in a smaller region in Ω_{m0}, $\Omega_{\Lambda 0}$ to construct the probability contour and extract the errors.

Figure 2 shows the 39%, 68%, 95% and 99% confidence level contours in the Ω_{m0}, $\Omega_{\Lambda 0}$ plane. Smooth contours have been obtained by the use of a Multi Layer Perceptrons (MLP) neural network [15, 16] with 2 hidden layers of 30 neurons each trained on the results of the fit. Position of the minimum and errors are given in line 3 of table 1.

The cosmological constant is found to be compatible with zero at a level better than 10^{-3}.

[5]DEC or Dark Energy Center is a HPC cluster of 800 cores funded by the OCEVU Labex (ANR-11-LABX-0060)

As a first consequence, the exotic redshift is similar to the standard one as it can be seen from equation 5.3. As a second consequence, the matter density becomes negative.

This is a well known effect. Fitting a curved universe with vanishing cosmological constant to the Hubble diagram entails a negative matter density that emulates the recent acceleration of the expansion of our universe. By comparing the χ^2's from line 1 and 3 in table 1 and using the log likelihood ratio statistical test hypothesis as in [18] we conclude that the exotic redshift is disfavored compared to the standard definition at a confidence level of at least 99.7%.

6 Conclusions

The confrontation of our exotic model with supernova data met with a – to the best of our knowledge – new challenge: in our model, the standardization of the absolute luminosities depends sensitively on the cosmological parameters. Therefore for every parameter choice we had to redo the global light curve fit for every supernova with the SALT2 procedure and our analysis required three and a half CPU years.

We had hoped that our exotic redshift would lower the mass density. It certainly did. However the obtained best fit for the exotic redshift is not good and its mass density negative. A negative mass density is not only physically problematic, it also is beyond the domain of validity of our perturbative solution, $Q+1 > 0$; a clean farewell to the exotic redshift, equation (4.3).

Acknowledgements: The project leading to this publication has received funding from Excellence Initiative of Aix-Marseille University - A*MIDEX, a French "Investissements d'Avenir" programme.

References

[1] M. Betoule *et al.* [SDSS Collaboration], "Improved cosmological constraints from a joint analysis of the SDSS-II and SNLS supernova samples," Astron. Astrophys. **568** (2014) A22 [arXiv:1401.4064 [astro-ph.CO]].

[2] K. Yu. Bliokh, A. Niv, V. Kleiner, E. Hasman, "Geometrodynamics of Spinning Light", Nature Photon. **2** (2008) 748. http://lanl.arxiv.org/abs/0810.2136, http://dx.doi.org/10.1103/PhysRevLett.96.073903

[3] W. G. Dixon, "Dynamics of Extended Bodies in General Relativity. I. Momentum and Angular Momentum", Proc. R. Soc. Lond. A **314** (1970). http://rspa.royalsocietypublishing.org/content/314/1519/499

[4] C. Duval, H. H. Fliche, J.-M. Souriau, "Un modèle de particule à spin dans le champ gravitationnel et électromagnétique", CRAS, **274** Série A (1972) 1082. http://gallica.bnf.fr/ark:/12148/bpt6k56190683/f60.image.r=Souriau?rk=42918;4

[5] C. Duval and T. Schücker, "Gravitational birefringence of light in Robertson-Walker cosmologies", arXiv:1610.00555 [gr-qc], Phys. Rev. D 96 (2017) 043517. http://dx.doi.org/10.1103/PhysRevD.96.043517

[6] F. I. Fedorov, "To the theory of total reflection", Doklady Akademii Nauk SSSR Vol. 105, # 3 (1955) 465. http://master.basnet.by/congress2011/symposium/spbi.pdf

[7] J. Guy *et al.* "SALT2: using distant supernovae to improve the use of Type Ia supernovae as distance indicators," Astron. Astrophys. **466** (2007) 11 [arXiv:astro-ph/0701828].

[8] O. Hosten, P. Kwiat, "Observation of the Spin Hall Effect of Light via Weak Measurements", Science **319**: 5864 (2008) 787–790. http://dx.doi.org/10.1126/science.1152697

[9] C. Imbert, "Calculation and Experimental Proof of the Transverse Shift Induced by Total Internal Reflection of a Circularly Polarized Light Beam", Phys. Rev. D **5** (1972) 787. http://dx.doi.org/10.1103/PhysRevD.5.787

[10] H. P. Künzle, "Canonical dynamics of spinning particles in gravitational and electromagnetic fields", J. Math. Phys. **13** (1972) 739. http://dx.doi.org/10.1063/1.1666045

[11] M. Mathisson, "Neue Mechanik materieller Systeme" Acta Phys. Pol. **6** (1937) 163; "Das zitternde Elektron und seine Dynamik", Acta Phys. Pol. **6** (1937) 218.

[12] A. Papapetrou, "Spinning Test-Particles in General Relativity. I", Proc. Roy. Soc. A **209** (1951) 248. http://rspa.royalsocietypublishing.org/content/209/1097/248

[13] R. V. Pound and G. A. Rebka, "Apparent weight of photons", Phys. Rev. Letters bf 3 (1960) 337.

[14] "The ROOT analysis package," http://root.cern.ch/drupal/

[15] F. Rosenblatt, "The perceptron: A probabilistic model for information storage and organization in the brain," Psychological Rev. **65** (1958) 386.

[16] "TMultiLayerPerceptron: Designing and using Multi-Layer Perceptrons with ROOT, " http://cp3.irmp.ucl.ac.be/ delaere/MLP/

[17] P. Saturnini, "Un modèle de particules à spin de masse nulle dans le champ de gravitation", Thèse de 3ème cycle en physique théorique, Université de Provence (1976). https://hal.archives-ouvertes.fr/tel-01344863v1

[18] T. Schücker and A. Tilquin, "Torsion, an alternative to the cosmological constant?," Int. J. Mod. Phys. D **21** (2012) 1250089 doi:10.1142/S0218271812500897 [arXiv:1109.4568 [astro-ph.CO]].

[19] J.-M. Souriau, "Modèle de particule à spin dans le champ électromagnétique et gravitationnel", Ann. Inst. Henri Poincaré **20 A** (1974), 315. http://www.jmsouriau.com/Publications/JMSouriau-ModPartSpin1974.pdf

[20] A. H. Taub, "Motion of Test Bodies in General Relativity", J. Math. Phys. **5** (1964) 112.

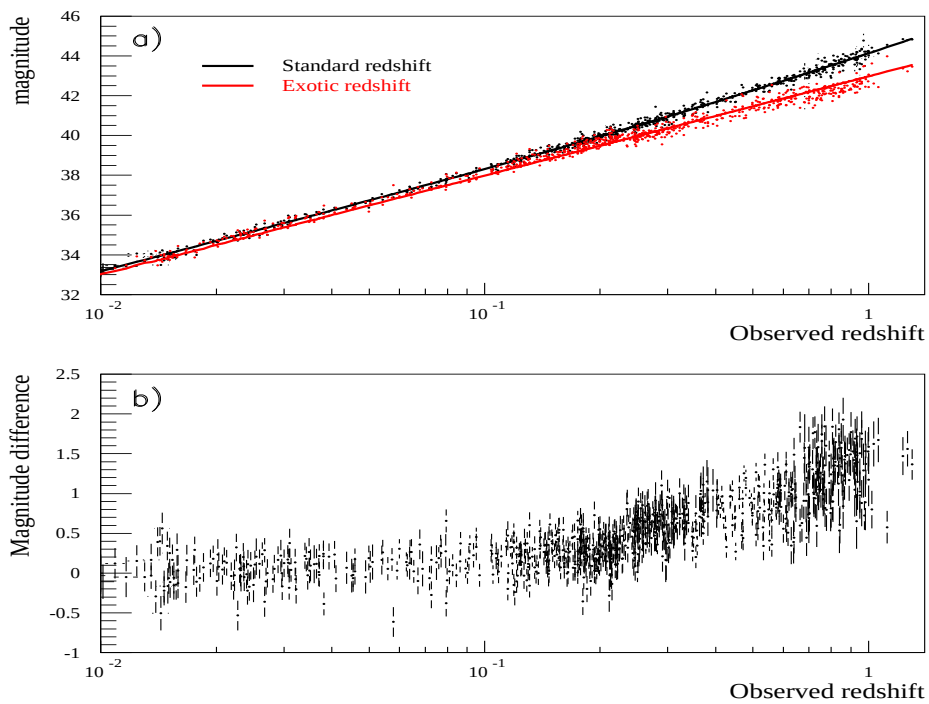

Figure 1: a) Hubble diagram with standard redshift in logarithmic scale (black points) and with exotic redshift (red points) at the same fiducial cosmology $\Omega_{m0} = 0.22$ *and* $\Omega_{\Lambda 0} = 0.63$ *artificially calibrated at the same low redshift magnitude. b) Relative difference in magnitude between standard and exotic redshifts after light curve re-fitting.*

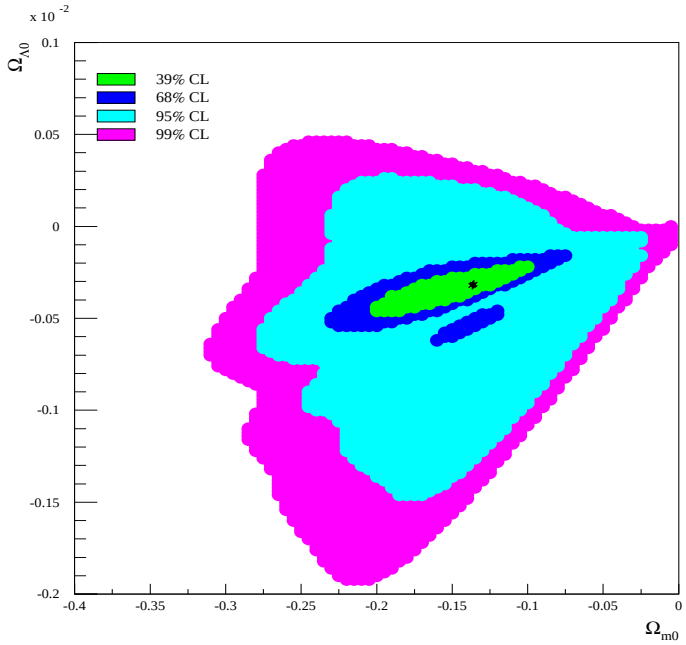

Figure 2: 39%, 68%, 95% *and* 99% *confidence level contours in the* Ω_{m0}, $\Omega_{\Lambda 0}$ *plane for exotic redshift. The black star shows the minimum at* $\Omega_{m0} = -0.15$ *and* $\Omega_{\Lambda 0} = -3.\,10^{-4}$.